Experimental validation of two semi-implicit homogeneous discretized differentiators on the CRAFT cable-driven parallel robot

Loic Michel, Marceau Métillon, Stéphane Caro, Malek Ghanes, Franck Plestan, Jean Pierre Barbot, Yannick Aoustin

Experimental validation of two semi-implicit homogeneous discretized differentiators on the *CRAFT* cable-driven parallel robot

L. Michel[a], M. Métillon[a], S. Caro[a], M. Ghanes[a], F. Plestan[a], J. P. Barbot[a], Y. Aoustin[b]

a. Laboratoire des Sciences du Numérique de Nantes, UMR CNRS 6004
1 rue de la Noë, BP 92101 F-44321 Nantes Cedex 3, France
Nantes Université, Ecole Centrale de Nantes,
b. Nantes Université,
loic.michel@ec-nantes.fr, marceau.metillon@ls2n.fr, stephane.caro@ls2n.fr,
malek.ghanes@ec-nantes.fr, franck.plestan@ec-nantes.fr, barbot@ensea.fr,
and Yannick.Aoustin@univ-nantes.fr

Résumé :

Ce travail est dédié à l'application de deux différentiateurs semi-implicites et homogènes pour estimer la vitesse de chacun des huit moteurs électriques du robot parallèle à câbles CRAFT à partir de l'enregistrement de la position angulaire de leur arbre de sortie respectif. Ces moteurs actionnent l'enroulement ou le déroulement de huit câbles pour déplacer la plateforme mobile du robot en translation et en rotation. Les résultats montrent que ces différentiateurs, dont les définitions sont fondées sur un et deux projecteurs, sont des outils performants pour estimer les vitesses angulaires des huit moteurs. Ces vitesses estimées sont beaucoup moins bruitées que leurs signaux de référence obtenus par différence arrière. Ces résultats laissent espérer un apport conséquent pour la commande du robot CRAFT.

Abstract :

This work is dedicated to the application of two differentiating homogeneous semi-implicit to estimate the angular velocity of each of the eight electric motors of the CRAFT cable-driven parallel robot from the recording of the angular position of their respective output shaft. These motors drive the winding or unwinding of eight cables to move the robot moving-platform. The results show that these differentiators, whose definitions are respectively based on one and two projectors, are extremely efficient tools for estimating the angular velocities of the eight motors. These estimated velocities are much less noisy than their reference signals obtained by backward difference. Those promising results will definitely contribute to a better control of the CRAFT robot.

Mots clefs : Robot parallèle à câbles, estimateur de vitesse, différentiateurs homogènes continus, différentiateurs homogènes discrets, semi-implicite discretisation d'Euler, projecteurs.

Keywords : cable-driven parallel robot, velocity estimation, homogeneous differentiators, homogeneous discretized differentiators, semi-implicit Euler discretization, projectors.

1 Introduction

A cable-driven parallel robot (CDPR) consists of a moving-platform that is connected to a rigid frame by means of cables and actuators, the latter being generally mounted on the ground. Most of the existing robots are powered by electric motors. These robots are very attractive for handling tasks [1, 2] because of their low inertia, a higher payload to weight ratio and a large workspace compared to conventional manipulator robots with articulated rigid limbs. Their possible application fields can be industrial, or dedicated to search-and-rescue operations. However, for tasks such as motion planning realized with CDPRs, haptic control is still improvable. To deal with various restrictions on cable tensions, cable elasticity, collisions and obstacle avoidance, over-actuation of the moving platform is actually a challenging scientific problem [3], [4].

As a consequence the control of CDPRs is challenging. One key point for their control design is the access, for each electric motor, to the angular variable and its time derivative of each actuator output shaft. These data are useful to design the robot control in tracking position or in haptic control [5]. Usually, the measurement of the angular variable of the output shaft of each actuator is made thanks to an encoder sensor or a resolver-to-digital converter. However, due to weight restrictions, reliability, and financial cost, a tachymeter is not usually available. A solution to get the value (or the estimation) of the angular velocities can be based on numerical differentiators. The expected characteristics of a differentiator are accuracy and low sensitivity to noise (the reader can refer to [6] for more details and state-of-the-art of differentiation solutions).

A CDPR, named *CRAFT* and located at LS2N, Centrale Nantes campus, is equipped with eight actuators and a moving-platform. Each motor has an encoder sensor measuring the angular velocity of its output shaft allowing to evaluate the performances of the differentiation solutions. The moving-platform has six degrees of freedom. This moving platform is thus over-actuated [7].

To estimate the velocity from the measured output motor shaft angles the design of continuous time differentiators can be a good way [8], [9]. However to be closer to physical systems, discretization differentiation is more convenient. The problem of digital differentiation is not new and several methods exist. Diop *et al* [10] investigate interpolation and numerical differentiation for constructing an approach to the design of nonlinear observers. The measured signal is sampled at discrete instants and interpolated by a polynomial for a window data. This elegant method is however not easy to apply in real time. Real-time discrete signal differentiation has been investigated with sliding-modes techniques. Reader can refer to [6] to obtain a good survey. The main problem to design digital differentiation is how to reject as much as possible the noise effects. Acary & Brogliato [11] introduced an implicit discretization technique, which overcome some limitations such as the chattering of the classical sliding-mode. They replace the sign function by an implicit projector. This very effective method has, however, a weakness in some areas, which will be explained in this paper. In the framework of the discrete homogeneous differentiation, the proposed differentiator combines explicit terms with implicit one including two *projectors* in order to reduce the effects of chattering is efficient [12] and [13]. This method was chosen to estimate the velocity of the *CRAFT* motors.

The performance of two new numerical differentiation schemes providing an estimation of the angular velocities is compared experimentally to the backward difference method. The first strategy is based

on a semi-implicit discretized homogeneous first-order differentiator [14] in the framework of velocity estimation regarding the angular variable of the actuator output shaft. The second strategy is based on a semi-implicit discretized homogeneous second-order differentiator [15] in the framework of velocity/acceleration estimation regarding the angular position. Those two differentiators combine an explicit differentiation part with an implicit differentiation one based on two *projectors* in order to reduce the effects of chattering phenomena as well as noise and disturbances. It should be noted that better performance was obtained with the two proposed differentiators compared to the backward difference scheme in terms of tracking errors and noise rejection.

The remaining of the paper is organized as follows. Section 2 is devoted to the presentation of *CRAFT* namely, its geometric, kinematic, and dynamic models. The problem is stated in Sec. 3 in order to present the homogeneous continuous-time differentiator. The semi-implicit Euler discretization is determined in Sec. 4. The experimental results are presented in Sec. 5. Conclusions and future work are drawn in Sec. 6.

2 The cable-driven parallel robot *CRAFT*

This section is dedicated to the description of *CRAFT* and its dynamic model.

2.1 *CRAFT* prototype located at LS2N, Nantes, France.

The cable-driven parallel robot prototype, named *CRAFT* is located at LS2N, France. The base frame of *CRAFT* is 4 m long, 3.5 m wide, and 2.7 m high, see Figure 1 a). The three-DoF translational and the three-DoF rotational motions of its suspended moving-platform (*MP*) are controlled with eight cables being respectively wound around eight actuated reels fixed to the ground. The *MP* is 0.28 m long, 0.28 m wide, and 0.2 m high, its overall mass being equal to 5 kg.

FIGURE 1 – *CRAFT*'s prototype located at LS2N, Nantes, France.

Figure 2 shows the main hardware of the prototype, which consists of a PC (equipped with © MATLAB and © ControlDesk software), eight © PARKER SME60 motors and TPD−M drivers, a © dSPACE DS1007-based real-time controller and eight custom made winches. Each cable can exert a tension up

to 150 N to the *MP*. The maximum velocity of each cable is equal to 5.9 m/s. The cable tensions are measured using eight FUTEK FSH04097 sensors, one for each cable, attached to cable anchor points. Their signal is amplified using eight FSH03863 voltage amplifiers and sent to the robot controller by a coaxial cable. Their measurement frequency is 1 kHz.

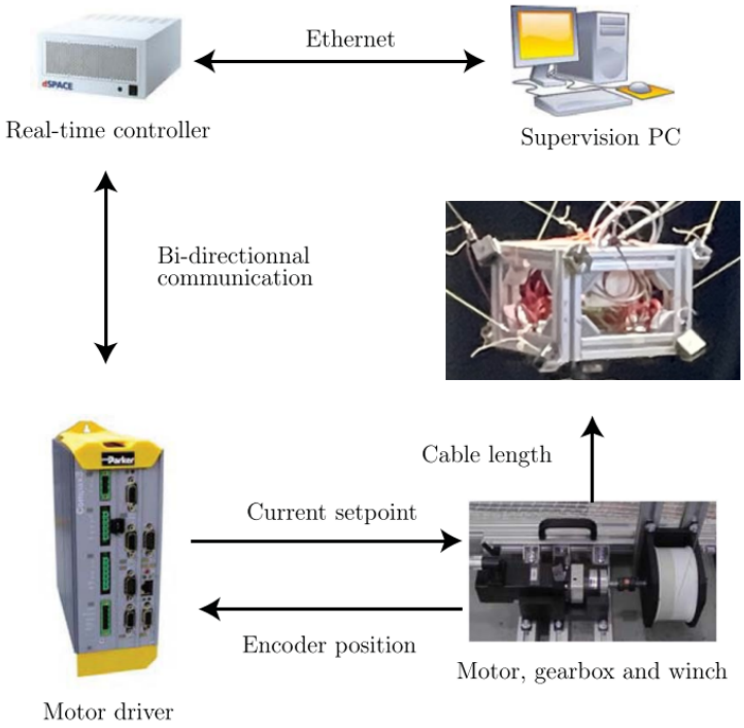

FIGURE 2 – The hardware of the prototype *CRAFT*.

2.2 Dynamic Model

The dynamic model of *CRAFT* expressed in this paper only considers the mass and inertia of the MP, the latter being pulled by the cables. Indeed, assuming that the diameters of the cables and the pulleys are small, the dynamic effects of the pulleys and the cables are neglected. A more general dynamic model taking into account also the dynamics of the motors, gearboxes, winches could also be considered, but would not provide fundamentally different information on the movement of the platform.

As described in [16] the dynamic equilibrium equation of the moving platform expressed as :

$$\mathbb{I}_p \ddot{\mathbf{p}} + \mathbf{C}\dot{\mathbf{p}} - \mathbf{w}_g = \mathbf{W}\tau + \mathbf{w}_e \tag{1}$$

where $\mathbf{W}$ is the wrench matrix that maps the cable tension vector τ into the wrench exerted by the cables onto the *MP*, and

$$\dot{\mathbf{p}} = \begin{bmatrix} \dot{\mathbf{t}} \\ \omega \end{bmatrix} \quad \ddot{\mathbf{p}} = \begin{bmatrix} \ddot{\mathbf{t}} \\ \alpha \end{bmatrix}, \tag{2}$$

where $\dot{\mathbf{t}} = [\dot{t}_x, \dot{t}_y, \dot{t}_z]^\top$ and $\ddot{\mathbf{t}} = [\ddot{t}_x, \ddot{t}_y, \ddot{t}_z]^\top$ are the vectors of the moving platform linear velocity and acceleration, respectively, while $\omega = [\omega_x, \omega_y, \omega_z]^\top$ and $\alpha = [\alpha_x, \alpha_y, \alpha_z]^\top$ are the vectors of the moving platform angular velocity and acceleration, respectively.

The external wrench $\mathbf{w}_e$ is a 6-dimensional vector expressed in the fixed reference frame $\mathscr{F}_b$ and takes the form

$$\mathbf{w}_e = \left[\mathbf{f}_e^\top, \mathbf{m}_e^\top\right]^\top = [f_x, f_y, f_z, m_x, m_y, m_z]^\top \tag{3}$$

f_x, f_y, and f_z are the x, y, and z components of the external force vector $\mathbf{f}_e$. m_x, m_y, and m_z are the x, y, and z components of the external moment vector $\mathbf{m}_e$, respectively. The components of the external wrench $\mathbf{w}_e$ are assumed to be bounded as follows

$$f_{min} \leq f_x, f_y, f_z \leq f_{max} \tag{4}$$

$$m_{min} \leq m_x, m_y, m_z \leq m_{max} \tag{5}$$

According to (4) and (5), the set $[\mathbf{w}_e]_r$, called the Required External Wrench Set (REWS), that the cables have to balance is a hyper-rectangle.

The *Center of Mass* (*CoM*) of the moving platform, G, may not coincide with the origin of the frame $\mathscr{F}_p$ attached to the platform. The mass of the platform being denoted by M, the wrench $\mathbf{w}_g$ due to the gravity acceleration vector $\mathbf{g}$ is defined as follows

$$\mathbf{w}_g = \begin{bmatrix} M\mathbf{I}_3 \\ \mathbf{M}\hat{\mathbf{S}}_p \end{bmatrix} \mathbf{g} \tag{6}$$

where $\mathbf{I}_3$ is the 3×3 identity matrix, $\mathbf{MS}_p = \mathbf{R}\,[Mx_p, My_p, Mz_p]^\top$ is the first momentum of the moving platform defined with respect to frame $\mathscr{F}_b$. The vector $\mathbf{S}_p = [x_p, y_p, z_p]^\top$ defines the position of G in frame $\mathscr{F}_p$. $\mathbf{M}\hat{\mathbf{S}}_p$ is the skew-symmetric matrix associated to $\mathbf{MS}_p$.

The matrix $\mathbb{I}_p$ represents the spatial inertia of the platform

$$\mathbb{I}_p = \begin{bmatrix} M\mathbf{I}_3 & -\mathbf{M}\hat{\mathbf{S}}_p \\ \mathbf{M}\hat{\mathbf{S}}_p & \mathbf{I}_p \end{bmatrix} \tag{7}$$

where $\mathbf{I}_p$ is the inertia tensor matrix of the moving-platform, which can be computed by the Huygens-Steiner theorem from the moving platform inertia tensor, $\mathbf{I}_g$, defined with respect to the platform *CoM*

$$\mathbf{I}_p = \mathbf{R}\mathbf{I}_g\mathbf{R}^\top - \frac{\mathbf{M}\hat{\mathbf{S}}_p\mathbf{M}\hat{\mathbf{S}}_p}{M} \tag{8}$$

$\mathbf{R}$ is the rotation matrix defining the moving-platform orientation and $\mathbf{C}$ is the matrix of the centrifugal and Coriolis wrenches, defined as

$$\mathbf{C}\dot{\mathbf{p}} = \begin{bmatrix} \hat{\omega}\hat{\omega}\mathbf{MS}_p \\ \hat{\omega}\mathbf{I}_p\omega \end{bmatrix} \tag{9}$$

where $\hat{\omega}$ is the skew-symmetric matrix associated to ω.

The 3D dynamic model of *CRAFT* is non-linear. In order to perform the most successful positioning or co-manipulation task, the knowledge of the robot state is necessary. *CRAFT* is not equipped of a sensor to measure the velocity of the output motor shaft angles. A numerical derivative of output motor shaft angles is thus required. In the following, a strategy is presented in order to obtain the numerical derivation of the output motor shaft angles.

3 Statement of the problem

The purpose is to estimate the velocity of the angular variable exclusively from the measured position of the output shaft for each of the eight motors. The continuous-time and the Euler implicit state models of the considered system are presented. Then the homogeneous continuous-time differentiator is introduced and its semi-implicit discretization is finally justified.

3.1 Continuous-time state model systems

Let $p(t)$ be a bounded perturbation, which is unknown such that there exists :

$$p_M > 0 \text{ such that } |p(t)| < p_M \text{ for all } t > 0. \tag{10}$$

The continuous model under consideration is the following one :

$$\Sigma : \begin{cases} \dot{x}_1 &= x_2 \\ \dot{x}_2 &= p(t) \\ y &= x_1 \end{cases} \tag{11}$$

where x_1 and x_2 are respectively the angular variable and its velocity ; y is the measure of x_1 with additional noise η.

Let the following notation be for the discretized variable :

$$\begin{array}{rcl} \bullet(t=(k+1)h) &=& \bullet^+ \\ \bullet(t=kh) &=& \bullet. \end{array} \tag{12}$$

The perturbation $p(t)$ is assumed to be a constant parameter or a slowly variable. This implies that for a sufficient small sampling-time $h > 0$, $p \equiv p^+$. As a consequence an implicit Euler discretization of the continuous-time model can be written with (12) as follows :

$$\begin{cases} x_1^+ = x_1 + hx_2^+ = x_1 + h(x_2 + hp^+) \\ x_2^+ = x_2 + hp^+ \\ y{=}x_1 \end{cases} . \tag{13}$$

3.2 Homogeneous continuous-time differentiator.

Homogeneity approach is very interesting because if for example a local stability is obtained due to the dilatation, this framework allows extending this local property to global settings, [17]. The option of a continuous-time homogeneous differentiator is therefore chosen under the assumption (10) [18], [19]. This differentiator can be written such as,

$$\begin{cases} \dot{z}_1 = z_2 + \lambda_1 \mu \lceil \varepsilon_1 \rfloor^\alpha \\ \dot{z}_2 = \lambda_2 \mu^2 \lceil \varepsilon_1 \rfloor^{2\alpha-1} \\ \hat{y} = z_1 \end{cases} \tag{14}$$

where $\alpha \in]0.5 \;\; 1[$ has to be fixed [20], $\varepsilon_1 = y - z_1$, and the notation $\lceil \bullet \rfloor^{\alpha} = |\bullet|^{\alpha}\text{sgn}(\bullet)$ is adopted along the paper. The degree of homogeneity of the differentiator (14) d is equal to $\alpha - 1$ with respect to dilatation Λ_r with $r = (r_1 = 1, r_2 = 1)$ [18]. Moreover, $\lambda_i > 0$, $i = 1, 2$ are the linear part gains, which are considered and allow to have the eigenvalues of the differentiation error ε_1 sufficiently stables, while the coefficient μ is chosen sufficiently large to cancel the effect of the unknown perturbation $p(t)$.

In order to be closer to the cable-driven parallel robot *CRAFT* and deal with real signal differentiation application, differentiators based on an Euler discretization approach will be designed in the next section.

3.3 Existing Euler discretization of the homogeneous continuous-time differentiator (14)

To design the Euler discretization of the homogeneous continuous-time differentiator (14) several solutions are possible and are obtained by using, explicit, implicit or semi-implicit methods. The semi-implicit method is is chosen in this paper for the following reasons.

Among the different Euler discretization methods two can be considered as follows :

— The usual explicit method : z_i and $\dot{z}_i$ for $i = 1, \; 2$ are known at $t = kh$ and z_i^+ is calculated such as.

$$z_i^+ = z_i + h\dot{z}_i \tag{15}$$

With (15) the explicit Euler discretization of the continuous-time differentiator (14) is deduced as follows,

$$\begin{cases} z_1^+ = z_1 + h\left(z_2 + \lambda_1 \mu \lceil \varepsilon_1 \rfloor^{\alpha}\right) \\ \\ z_2^+ = z_2 + h\lambda_2 \mu^2 \lceil \varepsilon_1 \rfloor^{2\alpha - 1}. \end{cases} \tag{16}$$

This model (16) unfortunately leads to a chattering effect and therefore the numerical solution is not attractive.

— Implicit method : z_i is known, $\dot{z}_i^+$ is chosen such that z^+ is equal to.

$$z_i^+ = z_i + h\dot{z}_i^+. \tag{17}$$

With (17) the implicit Euler discretization of the continuous-time differentiator (14) is deduced as follows,

$$\begin{cases} z_1^+ = z_1 + h\left(z_2^+ + \lambda_1 \mu \lceil \varepsilon_1^+ \rfloor^{\alpha}\right) \\ \\ z_2^+ = z_2 + h\lambda_2 \mu^2 \lceil \varepsilon_1^+ \rfloor^{2\alpha - 1}. \end{cases} \tag{18}$$

Observing the first equation of (18), if $\varepsilon_1^+ = 0$ then this implies that $z_2^+ = 0$. From the second equation the equality $z_2 = 0$ is deduced. The two correction terms $\lambda_1 \lceil \varepsilon_1^+ \rfloor^{\alpha}$ and $\lambda_2 \lceil \varepsilon_1^+ \rfloor^{2\alpha - 1}$ with $\varepsilon_1^+ = 0$ become inoperative.

A third approach, the semi-implicit homogeneous Euler discretization allows to overcome the drawbacks of these two previous numerical schemes, [12]. That is why this approach is chosen to discretize the continuous-time model (14). This is presented in the next section to design two variants of the semi-implicit homogeneous Euler differentiator.

4 Semi-implicit Homogeneous Euler differentiators

Two semi-implicit Euler discretization differentiators, defined with the acronyms SIHD-1 and SIHD-2 are considered [21]. For SIHD-1 the two correction terms are designed with the same projector, $\mathscr{N}_1$. Two projectors $\mathscr{N}_1$ and $\mathscr{N}_2$ are used respectively to design the correction terms with the differentiator SIHD-2.

4.1 Semi-implicit Euler homogeneous differentiator based on one projector (SIHD-1)

Considering the definition of the notation $\lceil \varepsilon_1^+ \rfloor \equiv |\varepsilon_1| \text{sign}(\varepsilon_1^+)$, the projector $\mathscr{N}_1$ is introduced in order to replace the function $\text{sign}(\varepsilon_1^+)$ as follows :

$$\begin{cases} z_1^+ = z_1 + h\left(z_2^+ + \lambda_1 \mu |\varepsilon_1|^\alpha \mathscr{N}_1\right) \\ \\ z_2^+ = z_2 + E_1^+ h \lambda_2 \mu^2 |\varepsilon_1|^{2\alpha-1} \mathscr{N}_1 \end{cases}. \tag{19}$$

Here the definition of the projector $\mathscr{N}_1$ and the tuning of the flag E_1^+ are such as :

$$\mathscr{N}_1(\varepsilon_1) := \begin{cases} \varepsilon_1 \in SD \ \ \rightarrow \mathscr{N}_1 = \dfrac{\lceil \varepsilon_1 \rfloor^{1-\alpha}}{\lambda_1 \mu h}, \ \ E_1^+ = 1 \\ \\ \varepsilon_1 \notin SD \ \ \rightarrow \mathscr{N}_1 = \text{sign}(\varepsilon_1), \ \ E_1^+ = 0, \end{cases} \tag{20}$$

with the domain of attraction $SD = \{\varepsilon_1 \,/\, |\varepsilon_1| \leq (\lambda_1 \mu h)^{\frac{1}{1-\alpha}}\}$.

Subtracting the first two equations of (19) from the first two equations of (13) leads to the following estimation error model :

$$\begin{cases} \varepsilon_1^+ = \varepsilon_1 + h\left(\varepsilon_2^+ - \lambda_1 \mu |\varepsilon_1|^\alpha \mathscr{N}_1\right) \\ \\ \varepsilon_2^+ = \varepsilon_2 + h\ddot{y} - E_1^+ h\left(\lambda_2 \mu^2 |\varepsilon_1|^{2\alpha-1} \mathscr{N}_1\right). \end{cases} \tag{21}$$

As a consequence we can remark from (21) that if $\varepsilon_1 \in SD$ then $\varepsilon_1 = h\varepsilon_2$.

4.2 Semi-implicit homogeneous Euler discretization based on two projectors (SIHD-2)

Here two different projectors, $\mathscr{N}_1$ and $\mathscr{N}_2$ are respectively used in order to control the estimation of z_1 and z_2. As a result, the semi-implicit homogeneous Euler discretization based on two projectors (SIHD-2) reads as :

$$\begin{cases} z_1^+ = z_1 + h\left(z_2^+ + \lambda_1 \mu |\varepsilon_1|^\alpha \mathscr{N}_1\right) \\ \\ z_2^+ = z_2 + E_1^+ h \lambda_2 \mu^2 |\varepsilon_1|^{2\alpha-1} \mathscr{N}_2. \end{cases} \tag{22}$$

Subtracting the first two equations of (26) from the first two of (13) leads to the following estimation error model :

$$\begin{cases} \varepsilon_1^+ = \varepsilon_1 + h\left(\varepsilon_2^+ - \lambda_1\mu|\varepsilon_1|^\alpha \mathscr{N}_1\right) \\ \\ \varepsilon_2^+ = \varepsilon_2 + h\ddot{y} - E_1^+ h\lambda_2\mu^2|\varepsilon_1|^{2\alpha-1}\mathscr{N}_2, \end{cases} \tag{23}$$

with the projector $\mathscr{N}_1$ and the flag E_1^+ defined in (20) and when $\varepsilon_1 \in SD$ the equality $\varepsilon_1 = h\varepsilon_2$ holds, $\mathscr{N}_2$ reads as :

$$\mathscr{N}_2 := \begin{cases} \varepsilon_1 \in SD' \rightarrow \mathscr{N}_2 = \dfrac{\lceil \varepsilon_1 \rfloor^{2(1-\alpha)}}{\lambda_2 h^2 \mu^2} \\ \\ \varepsilon_1 \notin SD' \rightarrow \mathscr{N}_2 = \text{sign}(\varepsilon_1), \end{cases} \tag{24}$$

where $SD' = \{\varepsilon_1 \in SD / |\varepsilon_1| \leq (\lambda_1\mu^2h^2)^{\frac{1}{2(1-\alpha)}} \equiv |\varepsilon_2| \leq (\lambda_1\mu^2)^{\frac{1}{2(1-\alpha)}} h^{\frac{\alpha}{1-\alpha}}\}$.

5 Experimental validation

5.1 Condition of data capture

For each of the eight electrical motors an encoder sensor measures the angular variable of its shaft. The eight motors are equipped with a gearbox reducer of ratio $n = 8$. The measured value is divided by n in order to obtain the angular position of the output shaft of the gearbox reducer. The robot *CRAFT* has no tachometer. The reference signal of the rotation velocity is thus obtained from the angular position by the backward difference calculation. The sampling period of the acquisition data is equal to 1 ms. The recording data in position and velocity are processed off-line in order to apply the semi-implicit homogeneous Euler discretized differentiators SIHD-1 and SIHD-2.

5.2 Attenuation noise projectors

The measured angular positions are noisy such as y becomes $y_m = x_1 + \eta$ where η is a measurement noise. The output corrective term e_1 becomes $e_{1m} = y_m - z_1$. As a consequence, a modified projector including a new parameter θ is introduced in order to mitigate the influence of noise. The semi-implicit Euler homogeneous differentiators SIHD-1 and SIHD 2 become :

SIHD-1

$$\begin{cases} z_1^+ = z_1 + h\left(z_2^+ + \lambda_1\mu|\varepsilon_{1m}|^\alpha \mathscr{N}_{\theta_1}\right) \\ \\ z_2^+ = z_2 + E_{\theta_1}^+ h\lambda_2\mu^2|\varepsilon_{1m}|^{2\alpha-1}\mathscr{N}_{\theta_1}, \end{cases} \tag{25}$$

$$\mathscr{N}_{\theta_1} := \begin{cases} (1-\theta)|\varepsilon_{1m}|^{1-\alpha} < \lambda_1\mu h \ \rightarrow \mathscr{N}_{\theta_1} = \dfrac{(1-\theta)\lceil \varepsilon_{1m} \rfloor^{1-\alpha}}{\lambda_1 h\mu} \\ \\ (1-\theta)|\varepsilon_{1m}|^{1-\alpha} \geq \lambda_1\mu h \ \rightarrow \mathscr{N}_{\theta_1} = \text{sign}(\varepsilon_{1\text{m}}) \end{cases}$$

SIHD-2

$$\begin{cases} z_1^+ = z_1 + h\left(z_2^+ + \lambda_1 \mu |\varepsilon_{1m}|^{\alpha} \mathscr{N}_{\theta_1}\right) \\ \\ z_2^+ = z_2 + E_{\theta_1}^+ h \lambda_2 \mu^2 |\varepsilon_{1m}|^{2\alpha-1} \mathscr{N}_{\theta_2}, \end{cases} \tag{26}$$

$$\mathscr{N}_{\theta_2} := \begin{cases} (1-\theta)\,|\varepsilon_{1m}|^{2(1-\alpha)} < \lambda_2 \mu^2 h^2 \rightarrow \mathscr{N}_{\theta_2} = \dfrac{(1-\theta)\lceil \varepsilon_{1m} \rfloor^{2(1-\alpha)}}{\lambda_2 h^2 \mu^2} \\ \\ (1-\theta)\,|\varepsilon_{1m}|^{2(1-\alpha)} \geq \lambda_2 \mu^2 h^2 \rightarrow \mathscr{N}_{\theta_2} = \mathrm{sign}(\varepsilon_{1\mathrm{m}}). \end{cases}$$

5.3 Determination of the semi-implicit Homogeneous Euler differentiator parameters

The λ_i, $i = 1,2$ parameters are chosen such as the linear part is stable. The value of homogeneous exponent α is chosen between the coefficient of Levant's differentiator ($\alpha^* = 0.5$) and the linear solution of the discretized differentiators SIHD-1 and SIHD-2 ($\alpha^* = 1$). The parameter θ is chosen by numerical test trial and error allowing a good filtering of the noise *i.e.* $0.5 < \theta < 1$. This parameter can been refined thanks to an optimization procedure minimizing a criterion, which is based on the 2-norm of the estimation error in velocity. The μ parameter is also chosen by numerical test trial and error in order to determine the best possible action of both projectors $\mathscr{N}_{\theta i}$. The numerical values of these five parameters are tuned as follows :

$$\lambda_1 = 2\ 10^4, \quad \lambda_2 = 1\ 10^4, \quad \alpha = 0.81, \quad \theta = 0.9, \quad \mu = 1. \tag{27}$$

5.4 Discussion about the experimental results

Figure 3, presents for the eight motors the recording angular positions of the output shaft, which supports the winch, after the gearbox, and the associate velocities calculated by backward difference. These reference velocities are compared with the results from both semi-implicit Euler differentiators SIHD-1 and SIHD-2. The performances of these differentiators are quasi uniform whatever the motors. The angular velocities are smoother *i.e.* less noisy than the reference velocities obtained by backward difference and more specifically a backward difference numerical scheme. The dynamics of the three signals are similar. No delay can be identified between the signals. However it is noteworthy that the transient behavior of the velocity, which is obtained with the semi-implicit homogeneous Euler differentiator SIHD-2 is better than the one obtained with the semi-implicit homogeneous Euler differentiator SIHD-1. As there is no tachymeter sensor on the motor shaft it is difficult to present the backward difference as the one that gives the reference angular velocity. Nevertheless, we can evaluate each of the angular velocity signal in terms of their sensitivity to noise. In a common time window, which is equal to 29s-31s we determined the standard deviation of the angular velocities estimated with the SIHD-1 and SHID-2 methods ; the velocity calculated by the Backward difference method. Table shows the result for the fourth motor, which represents quite well the general behavior for the eight motors. The sensitivity to noise is much lower for the angular velocity signals with the SIHD-1 and SHID-2 methods than with the backward difference.

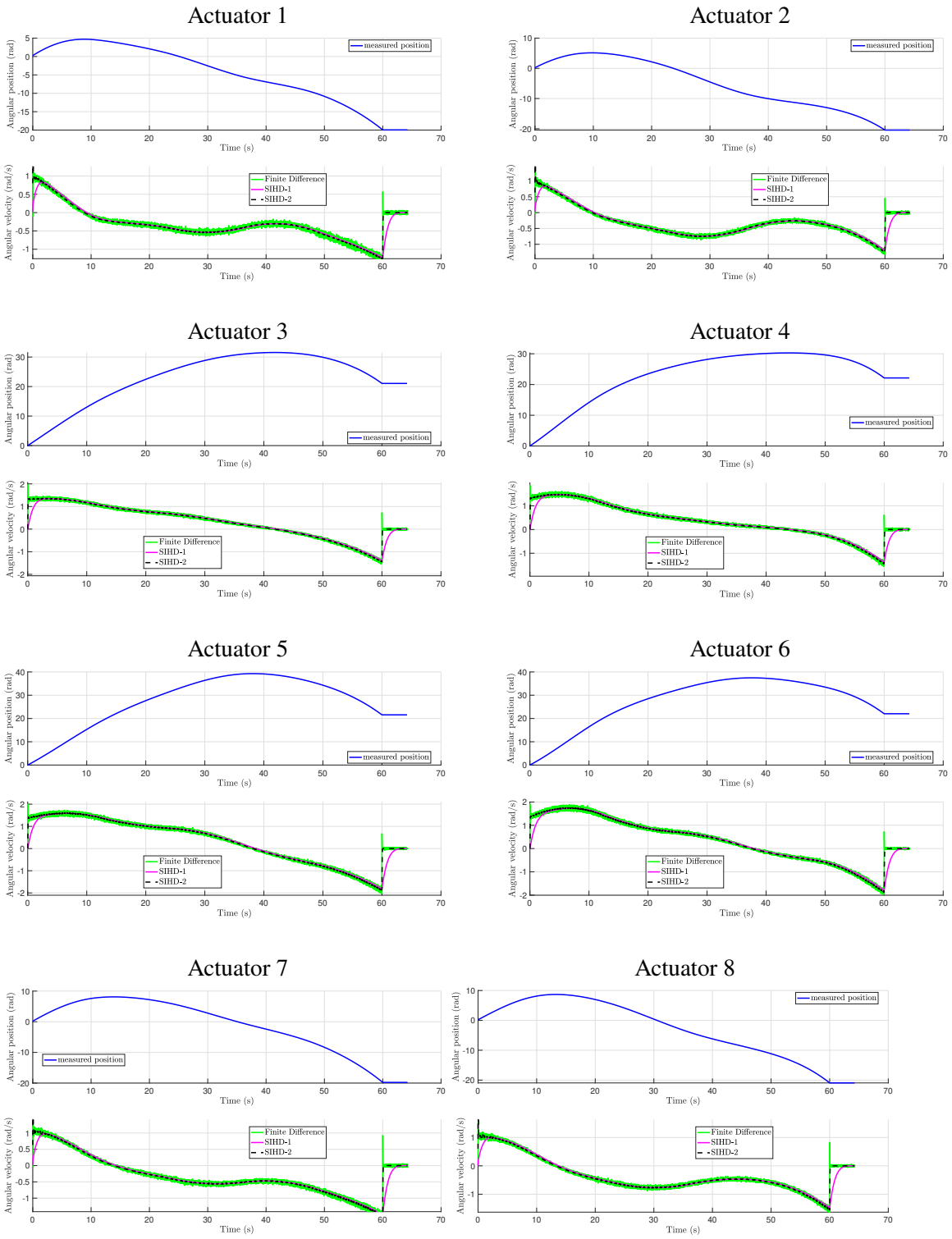

FIGURE 3 – Experimental data for the eight motors : Recording angular positions (blue color), reference velocity calculated by backward difference (green color), estimated velocities with differentiator SIHD-1 (solid line red color) and estimated velocities with differentiator SIHD-2 (dashed line black color).

	angular velocity (rad/s)		
	σ, BD	σ, SIHD-1	σ SIHD2
motor 4	0.032	0.017	0.017

Table : Standard deviation to evaluate the noise for velocity of the fourth motor.

6 Conclusion

The cable-driven parallel robot *CRAFT* is a complex mechanical system for which the control is difficult due to its over-actuated nature and cable tension constraints. However, its future is promising for applications such as handling, rescue or personal assistance. Two new semi-implicit homogeneous differentiators are applied with success to estimate the angular velocity of the output shaft of the eight motors of the robot *CRAFT*. The obtained velocities are less noisy that the one calculated with backward difference.

The results open a great perspective window for the family of robots. First the application of semi-implicit homogeneous differentiators for identification tasks of model parameters such as Coulomb or kinematic frictions, inertia moments, masses could be very efficient. Secondly one important task of a cable-driven parallel robot is the co-manipulation between its effector and human thanks a force sensor. From the measure of a force sensor, a mass parameter allows to deduce an acceleration vector. After a double integration of this acceleration vector a Cartesian trajectory is deduced. Finally a reference trajectory for each motor can be deduced thanks an inverse geometric model and an inverse kinematic model [5]. The tracking of these reference trajectories has to be perfect with high gain values. As a consequence the semi-implicit homogeneous differentiators SIHD-1 or SIHD-2 can be very useful for the control task.

Acknowledgment

This work is supported by the ANR project DigitSlid ANR-18-CE40-0008-01 (https ://anr.fr/Project-ANR-18-CE40-0008) ; the ANR CRAFT project, grant ANR-18-CE10-0004 (https ://anr.fr/Project-ANR-18-CE10-0004). The research work was also motivated by the EquipEx+ TIRREX project, grant ANR-21-ESRE-0015 (https ://www.ls2n.fr/le-projet-tirrex-est-laureat-de-lami-equipex/).

Références

[1] E. Picard, S. Caro, F. Plestan, F. Claveau, Control Solution for a Cable-Driven Parallel Robot with Highly Variable Payload, in : ASME 2018 International Design Engineering Technical Conferences Computers and Information in Engineering Conference IDETC/CIE 2018, no. DETC2018-85304, Quebec city, Canada, 2018, pp. 1429–1436.
URL https://hal.archives-ouvertes.fr/hal-01863730

[2] E. Picard, F. Plestan, E. Tahoumi, F. Claveau, S. Caro, Control Strategies for a Cable-Driven Parallel Robot with Varying Payload Information, Mechatronics 79 (2021) 102648.
URL https://hal.archives-ouvertes.fr/hal-03332227

[3] M. Gouttefarde, J.-F. Collard, N. Riehl, C. Baradat, Geometry selection of a redundantly actuated cable-suspended parallel robot, IEEE Transactions on Robotics 31 (2) (2015) 501–510.

[4] H. Hussein, J. C. Santos, J.-B. Izard, M. Gouttefarde, Smallest maximum cable tension determination for cable-driven parallel robots, IEEE Transactions on Robotics 37 (4) (2021) 1186–1205.

[5] P. Lemoine, P. P. Robet, M. Gautier, C. Damien, Y. Aoustin, Haptic control of the parallel robot orthoglide, in : 2019 in Proc of the 24td Congrès Français de Mécanique, CFM, Brest, France, 26-30 August, 2019.

[6] M. R. Mojallizadeh, B. Brogliato, A. Polyakov, S. Selvarajan, L. Michel, F. Plestan, M. Ghanes, J.-P. Barbot, Y. Aoustin, Discrete-time differentiators in closed-loop control systems : experiments on electro-pneumatic system and rotary inverted pendulum, HAL-INRIA [Research Report hal-031225960] (2021).

[7] U. A. Mishra, M. Métillon, S. Caro, Kinematic stability based afg-rrt* path planning for cable-driven parallel robots, in : IEEE International Conference on Robotics and Automation ICRA, Xi'an, China, 2021.

[8] A. Levant, Robust exact differentiation via sliding mode technique, automatica 34 (3) (1998) 379–384.

[9] A. Levant, Sliding order and sliding accuracy in sliding mode control, Int. J. of control 58 (6) (1993) 1247–1263.

[10] S. Diop, J. Grizzle, P. Moraal, A. Stefanopoulou, Interpolation and numerical differentiation for observer design, in : Proceedings of 1994 American Control Conference - ACC '94, Vol. 2, 1994, pp. 1329–1333 vol.2. doi:10.1109/ACC.1994.752275.

[11] V. Acary, B. Brogliato, Y. V. Orlov, Chattering-free digital sliding-mode control with state observer and disturbance rejection, IEEE Trans. on Automatic Control 57 (5) (2012) 1087–1101.

[12] L. Michel, M. Ghanes, F. Plestan, Y. Aoustin, J. Barbot, Semi-implicit Euler discretization for homogeneous observer-based control : one dimensional case, in : Proc. of the IFAC-V 2020, World Congress, Berlin, Germany, 2020.

[13] L. Michel, S. Selvarajan, M. Ghanes, F. Plestan, Y. Aoustin, J. P. Barbot, An experimental investigation of discretized homogeneous differentiators : pneumatic actuator case, IEEE Journal of Emerging and Selected Topics in Industrial Electronics 2 (3) (2021) 227–236. doi:10.1109/JESTIE.2021.3061924.

[14] L. Michel, S. Selvarajan, M. Ghanes, F. Plestan, Y. Aoustin, J.-P. Barbot, An experimental investigation of discretized homogeneous differentiators : Pneumatic actuator case, IEEE Journal of Emerging and Selected Topics in Industrial Electronics 2 (3) (2021) 227–236.

[15] L. Michel, M. Ghanes, F. Plestan, Y. Aoustin, J.-P. Barbot, Semi-implicit homogeneous euler differentiator for a second-order system : Validation on real data, in : IEEE Control and Decision Conference CDC, Austin, Texas, USA, 2021.

[16] L. Gagliardini, M. Gouttefarde, S. Caro, Determination of a dynamic feasible workspace for cable-driven parallel robots, Proceedings in Advanced Robotics, Springer, 2016, pp. 361–370.

[17] L. Rosier, Homogeneous lyapunov function for homogeneous continuous vector field, Systems & Control Letters 19 (6) (1992) 467–473.

[18] W. Perruquetti, T. Floquet, E. Moulay, Finite-time observers : application to secure communication, IEEE Trans. on Automatic Control 53 (1) (2008) 356–360.

[19] M. Ghanes, J. P. Barbot, L. Fridman, A. Levant, R. Boisliveau, A new varying-gain-exponent-based differentiator/observer : An efficient balance between linear and sliding-mode algorithms, IEEE Trans. on Automatic Control 65 (12) (2020) 5407–5414.

[20] Y. Hong, J. Huang, Y. Xu, On an output feedback finite-time stabilization problem, IEEE Transactions on Automatic Control 46 (2) (2001) 305–309. doi:10.1109/9.905699.

[21] L. Michel, M. Ghanes, F. Plestan, Y. Aoustin, J. Barbot, Semi-implicit homogeneous Euler differentiator for a second-ordersystem (2020).